



Single-Crystalline Silicon Nanowire Array-Based Photoelectrochemical Cells

Enrique A. Dalchiele,^{a,*} Francisco Martín,^b Dietmar Leinen,^b
Ricardo E. Marotti,^a and José Ramón Ramos-Barrado^{b,*}

^aInstituto de Física, Facultad de Ingeniería, Universidad de la República, 11000 Montevideo, Uruguay

^bLaboratorio de Materiales y Superficie (Unidad Asociada al CSIC), Departamentos de Física Aplicada & Ingeniería Química, Universidad de Málaga, E29071 Málaga, Spain

Single-crystalline n-type silicon nanowire (n-SiNW) arrays have been synthesized by electroless metal deposition on a silicon wafer chip in an ionic Ag/HF solution through selective etching. The photoelectrochemical properties of the SiNW arrays were studied (under 40 mW cm⁻² white illumination conditions) in an aqueous electrolyte [with Fe(CN)₆⁴⁻/Fe(CN)₆³⁻ redox couple] and compared to those of its untreated bare polished Si sample counterpart (n-Si). The open-circuit photovoltage was lower, on average, for SiNWs array photoelectrodes, while short-circuit current density, fill factor, and overall energy conversion efficiency of the SiNWs array photoelectrodes were generally superior to those of the n-Si junction devices.

© 2009 The Electrochemical Society. [DOI: 10.1149/1.3089318] All rights reserved.

Manuscript submitted October 7, 2008; revised manuscript received January 14, 2009. Published March 10, 2009.

Silicon (Si) is, for excellence, the most important semiconductor material since the Si-based devices have dominated microelectronic technology for many decades.^{1,2} Besides this, low-dimensional nanomaterials are of particular interest because they may exhibit anisotropic or dimension tunable properties, both of which are important attributes in nanodevice applications.² In the last few years, silicon nanowires (SiNWs) have attracted much attention because of their unique properties and their compatibility with the Si-based microelectronics. Then, SiNWs are attractive for applications in field-emission devices, chemical sensors, spintronics, and photonics.

More recently, much attention has appeared on the use of low-dimensional semiconductor nanostructures, especially one-dimensional (1D) semiconductor nanorods and nanowires, for the optimization of the photovoltaic energy conversion and reducing cost issues in solar cells.³⁻¹⁰ The approach to attempt those scopes is based on the orthogonalization of the directions of light absorption and charge-carrier collection.¹¹⁻¹³ For instance, the semiconducting absorber comprised of a vertically oriented array of high-aspect ratio nanowires could, in principle, provide sufficient optical absorption along its axial dimension, while facilitating collection of carriers radially over a distance sufficiently short to compensate for a short minority carrier collection length (if an inexpensive, i.e., not totally pure absorber material uses low-quality materials).⁹⁻¹³ In particular, for an absorber material that is carrier-collection limited and does not have an excessively high rate of depletion-region recombination, the analysis of the device physics (generation, transport, and recombination equations) has shown that such nanorod arrays can potentially offer improved performance relative to traditional planar junctions.^{9,12,13} Moreover, all those concepts and considerations that have been described above can, in principle, be extrapolated to the photoelectrochemical (PEC) liquid junction solar cells case. For instance, ZnO nanowire- and nanorod-based dye-sensitized solar cells have been produced,^{4,14} and photoresponse studies toward the water-splitting reaction on n-TiO₂ nanowire electrodes have been reported.¹⁴ In particular, a very interesting and exhaustive study comparing the PEC behavior of nanorod array and planar thin-film Cd(Se,Te) photoelectrodes has recently been reported.¹¹ However, comparatively little work has been performed on the use of SiNWs array as photoelectrodes in PEC solar cells. It must be pointed out that research on SiNW-based solid-state solar cells is also still in "its infancy," as was expressed by Stelzner et al. in a paper reporting results on SiNW-based solar cells.¹⁵ To date, in this way and regarding PEC study of SiNWs, only some works have appeared, to our

knowledge only three.¹⁶⁻¹⁸ Two of them reporting the preparation and characterization of PEC cells based on vapor-liquid-solid (VLS)-grown silicon nanorods (2 μm diam) arrays¹⁶ and VLS-grown SiNWs (57 nm diam) arrays¹⁷ have been published in the last year. It is also worth noting that in the VLS process, complex equipment and rigorous conditions (high temperature and high pressure) are often required, limiting their further applications. However, in the last years, the electroless metal deposition (EMD) method has been proposed to growth SiNWs,¹⁹ which partially overcame VLS method shortcomings (as unusual conditions, such as high pressure, are still needed in the EMD procedure). Only very recently, and during the preparation of the present manuscript, a work reporting the performance of a PEC solar cell based on SiNW arrays prepared by EMD etching performed at high pressure has appeared.¹⁸ Moreover, this PEC study has been carried out in a Br⁻/Br₂ redox electrolyte solution and in a two-electrode system.

In the present work, n-type silicon nanowires (n-SiNW) arrays have been synthesized by EMD performed at near room temperature and under normal pressure conditions (1 atmosphere pressure), on a silicon wafer chip in an ionic silver HF solution through selective etching.²⁰ Electroless metal deposition in an ionic metal (silver in the present work) HF solution is based on microelectrochemical redox reaction in which both anodic and cathodic processes occur simultaneously at the silicon surface. This fabrication method offers several advantages with respect to other preparation techniques of SiNWs (for example, VLS): (i) Because the as-prepared SiNWs are an integral part of the silicon wafer substrate, they provide an uninterrupted electronic pathway (i.e., SiNWs have a direct, high-quality electrical contact with the underlying silicon substrate); (ii) the SiNWs have direct 1D electronic pathways allowing for efficient charge transport; and (iii) the SiNWs directly inherit the electrical properties from the bulk silicon substrate; thus, there is no need of further doping for conductivity control. Moreover, the PEC properties of the SiNW arrays were studied in an aqueous electrolyte [with Fe(CN)₆⁴⁻/Fe(CN)₆³⁻ redox couple], and compared to those of its untreated bare polished Si sample counterpart.

Experimental

Single-side polished Si(100) wafer chips (TOPSIL), 500 μm thick, n-doped (9–15 Ω cm resistivity) with approximate areas of 1 cm², were first washed in boiling acetone for 10 min and, subsequently, in isopropanol at room temperature, with sonication for 5 min. They were oxidized in H₂O₂/HCl/H₂O (2:1:8) at 353 K for 15 min to remove any trace of heavy metals and organic species, rinsed copiously with deionized (DI) water, etched with 10% aqueous HF for 10 min, rinsed with water again, dried under a stream of N₂, and immediately used in either as a substrate in the SiNW growth process or in the preparation of the planar polished n-Si(100)

* Electrochemical Society Active Member.

^z E-mail: dalchiel@fing.edu.uy

photoelectrodes. The n-SiNW arrays have been synthesized by EMD on the silicon wafer chips in an ionic silver HF solution through selective etching. The cleaned Si wafer chips were immersed into an aqueous HF/AgNO₃ solution for 15–30 min at 50°C (the concentration of HF and AgNO₃ here are chosen to be 4.6 and 0.02 M, respectively). The length of SiNWs could be effectively controlled through tuning the treatment time. After the treatment, the as-synthesized samples were rinsed copiously in DI water and dried at room temperature. Then, the SiNW arrays were dipped in 30 wt % HNO₃ aqueous solution for 60 s and repeated for several times to remove all residual Ag from the nanowire surfaces. After the nitric acid bath, no Ag peaks appeared in the X-ray photoelectron spectroscopy (XPS) spectra of the nanowires.²⁰ Eventually, and in order to prepare the planar polished n-Si and SiNW array photoelectrodes, ohmic contact was made to the back of the polished n-Si and SiNW samples by scratching the Si surface, rubbing it with Ga–In eutectic, and attaching a copper contact to it. The edges of the silicon squares and the copper were isolated with an adhesive Teflon tape leaving a defined exposed area of 0.196 cm² facing the solution. Before the electrochemical experiments, the electrode surface was again etched for 15 min with the 10% aqueous HF solution (after this procedure, an atomically smooth and hydrogen terminated surface has been obtained).

Scanning electron microscopy (SEM) pictures were obtained with a JEOL JSM-5410 apparatus. Transmission electron microscopy (TEM) and selected area electron diffraction (SAED) were carried out with a Philips CM-200 microscope operated at 200 kV. Specimens for TEM were prepared by removing the electrodeposited material by grating with a scalpel, collected, and ultrasonically dispersed in 1 mL of ethanol. A small drop of the suspended solution was placed onto a porous carbon film supported on a TEM nickel grid and was dried in air prior to observation.

Optical reflectance spectra between 400 and 900 nm were measured with an S2000 Ocean Optics spectrophotometer. Absolute specular reflectance at 633 nm was measured at 45°, illuminating by means of a He–Ne ORIEL 10 mW nominal power laser and with the use of an ORIEL 70260 Power Meter using a ORIEL 70282 photodiode detector.

PEC studies were carried out in a three-armed cell with a platinum counter electrode and saturated calomel electrode (SCE) as reference. All potential values in this article are reported vs this reference electrode. These PEC studies have been performed in a 0.5 M KNO₃ + 0.1 M K₃Fe(CN)₆ + 0.1 M K₄Fe(CN)₆ solution. All solutions were prepared from analytical grade reagents and 18 MΩ cm Millipore water. The electrolyte solutions were purged with nitrogen for 30 min prior to each experimental series and then kept under flowing nitrogen during the experiments. A 200 W tungsten-halogen lamp (ORIEL) was used as the light source. The incident power at the electrode surface was determined as 40 mW/cm² (using a previously calibrated solar cell with a Kipp&Zonen piranometer), after eliminating the light reflection and absorption effects at the Pyrex glass cell and electrolyte, respectively. The PEC performance of the n-Si and n-SiNWs photoelectrodes has been assessed by using linear sweep voltammetry both in the dark and under illumination by using an AUTOLAB Electrochemical Analyzer (model PGSTAT 30, Eco Chemie BV, The Netherlands).

The photocurrent-time dependence (photocurrent transient experiments) under constant external bias and intermittent illumination (hand-chopped light) was carried out with the same PEC experimental setup described above.

Results and Discussion

The SEM image of a typical as-prepared SiNW array (30 min etching) is shown in Fig. 1, which shows the cross-sectional details of the SiNW array in which all SiNWs are distinguishable, and most of them are vertical to the wafer surface, exhibiting a length ~30 μm and diameters in the range of 100–160 nm. Some disorder SiNWs arise from cutting and loading of the SEM sample. The

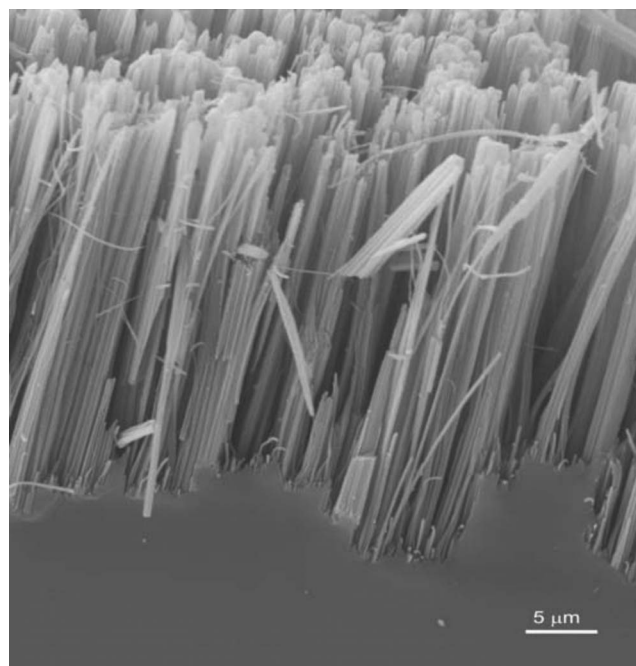


Figure 1. Typical SEM cross-sectional image of SiNW arrays produced on 9–15 Ω cm n-Si(100) substrate in 4.6 M HF/0.02 M AgNO₃ at 50°C.

density of SiNW arrays is ~10⁹/cm². Figure 2 shows a high-resolution TEM image of a typical SiNW of ca. 155 nm diam and with a rough surface. This roughness may be attributed to randomness of the lateral oxidation and etching in the HF aqueous solution, or a faceting of the lattice during the synthesis due to a low HF etching.²¹ The nanowires were single crystalline, as shown by the high-resolution TEM image of the Si lattice of an EMD SiNW (see Fig. 2), and by the SAED pattern (inset of Fig. 2).

The SiNW array samples are black in appearance and nonreflective. In effect, the image in the inset of Fig. 3 is a photograph that

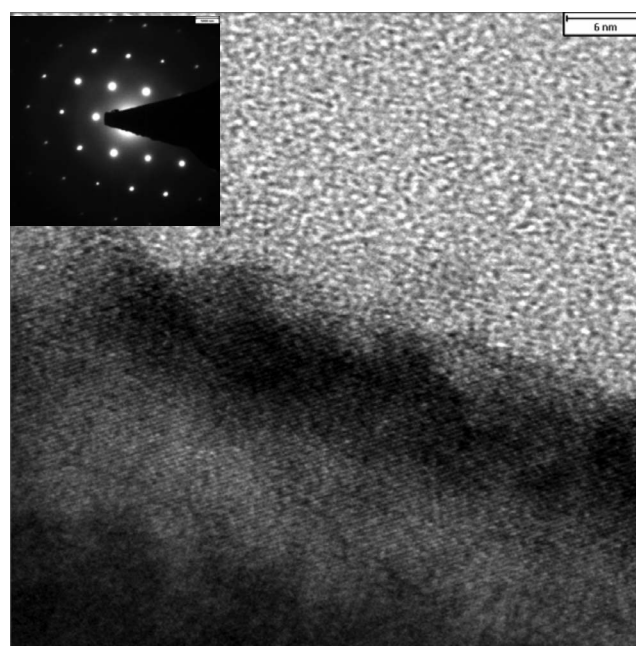


Figure 2. HRTEM image of a single SiNW. Inset shows the corresponding electron diffraction pattern. SiNWs prepared as in Fig. 1.

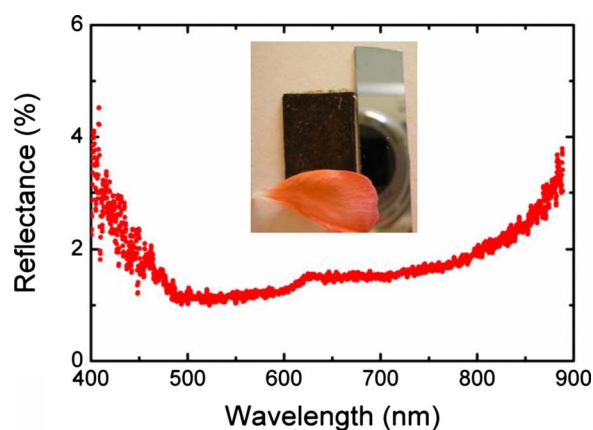


Figure 3. (Color online) Optical reflectance spectrum for n-SiNW array samples normalized to the maximum reflectance of a bare silicon sample. Inset shows a picture of an n-SiNW array Si wafer chip sample (5 cm²) (left), showing its dark, nonreflective, and matte appearance; and a bare polished n-Si (right).

compares the view (to the naked eye) of the nanowire array with the one of a bare polished n-Si. Although this last one is almost specular, the former one is dark black and nonreflective. Figure 3 shows the optical reflectance spectrum of the SiNW array samples normalized to the maximum reflectance of a bare silicon sample. The reflectance of the SiNW array is <5% smaller than the one of the bare polished n-Si sample, in the whole measured spectra. In either case, no clear structure can be found. The increase of the reflectance to the IR and UV may still be due to the normalization process. There is a small structure at ~620 nm (red spectral region), which lead to a further diminishing of the visible reflectance. This kind of structure has been observed in Ref. 7 and may be attributed to absorption and scattering of light due to the size and shape of the nanowires.²² To quantify the total reflectance, the specular absolute reflectance was measured at 633 nm with the use of a He-Ne laser. From the most uniform samples, this absolute specular reflectance was found between 0.4 and 0.7%, in accordance with their opaque black appearance. These very low reflectance values are almost comparable to the diffuse reflectance, which increases due to the light scattering originated in the rough surface of the SiNW samples. The dark appearance of the SiNW is not only a consequence of their rough surfaces, which scatters incoming light, increasing light absorption because of multireflection process, such as in a standard blackbody, but also multi-antireflection and light trapping effects arising in the nanowire array have recently been claimed.^{18,23}

The junction properties of such SiNW arrays were explored using a liquid electrolyte (in a PEC system). The use of a liquid junction provided a high-quality, conformal, and rectifying contact to the Si nanowires,^{11,16,24} hence, allowing measurements of the performance of the SiNWs without requiring a diffused metallurgical junction to the SiNW array.^{11,16,24} Moreover, a direct comparison between the PEC performance of a clean polished n-Si(100) (planar) (with the same electrical characteristics, i.e., doping concentration, as the silicon wafer chip substrate where the SiNWs have been grown) and the synthesized SiNWs array photoelectrodes has been done. For our purposes, the liquid used for contact must contain a well-behaved redox couple and be a sufficiently good conductor to ensure well-defined electrochemical behavior. The n-type Si is among the n-type semiconductors that undergo photoanodic reactions;²⁵ in fact, in aqueous solutions, the surface of the silicon photoanode is readily oxidized (i.e., photocorrosion).²⁶ Thus, for applications in PEC cells, the semiconductor surface should be stabilized against photocorrosion. Photocorrosion is generally associated with the reaction of photogenerated holes with surface atoms and can be minimized by providing a suitable hole-capturing agent in the solution. Toward this end, Madou et al. reported high-

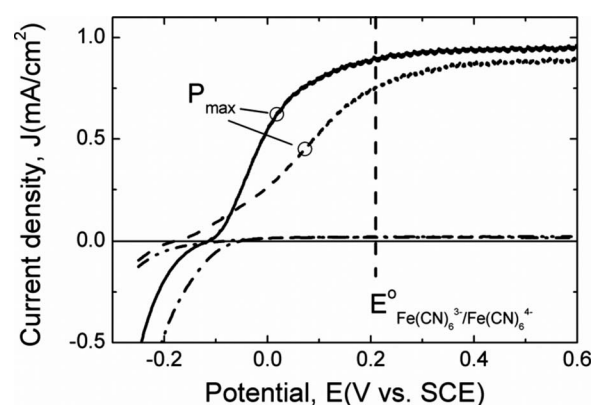


Figure 4. Steady-state current density-voltage characteristics for typical n-SiNW array and clean polished n-Si photoelectrodes in 0.5 M KNO₃ + 0.1 M K₃Fe(CN)₆ + 0.1 M K₄Fe(CN)₆ solution in the dark and under white illumination (40 mW/cm²). The potential scan rate is 10 mV/s. The solid and the dashed-dotted lines are the behavior of the n-SiNW array photoelectrode under illumination and in the dark, respectively. The dashed and the dashed-double dotted lines are the behavior of the polished n-Si photoelectrodes under illumination and in the dark, respectively. The equilibrium formal redox potential ($E^{\circ} = 0.209$ V vs SCE) for the $[\text{Fe}(\text{CN})_6]^{3-/4-}$ redox couple is also indicated.

stabilization efficiencies in 0.1 M K₄Fe(CN)₆ + 0.5 M KCl solution.²⁶ Consequently, herein the $\text{Fe}(\text{CN})_6^{4-}/\text{Fe}(\text{CN})_6^{3-}$ redox couple has been selected, and the PEC studies have been performed in a 0.5 M KNO₃ + 0.1 M K₃Fe(CN)₆ + 0.1 M K₄Fe(CN)₆ solution. PEC measurements were performed in a conventional three-electrode PEC cell, with a platinum counter electrode and a SCE (all potentials in the present work are given with respect to this electrode). The light source was a 150 W tungsten-halogen lamp being the intensity arriving at the electrode surface of 40 mW/cm², after being corrected for interface reflection and for solution absorption losses. The PEC performance of the n-Si and n-SiNWs photoelectrodes has been assessed by using linear sweep voltammetry both in the dark and under illumination. With this procedure, it can be evaluated both the “dark” electrochemical behavior and the PEC response. Figure 4 shows typical steady-state j - E characteristics both in the dark and under 40 mW/cm² white illumination of polished n-Si and n-SiNW (etching time 15 min) array photoelectrodes in the 0.1/0.1 M $\text{Fe}(\text{CN})_6^{4-}/\text{Fe}(\text{CN})_6^{3-}$ solution with $E^{\circ} = 0.209$ V vs SCE. Here, the potential was swept from cathodic to anodic direction, and the curves were obtained immediately after etching the electrodes in a 10% HF solution for 10 min. In dark conditions, and as was expected, both electrodes exhibited n-type behavior, passing cathodic current at forward bias and showing a very good rectification toward anodic current flow. Therefore, under illumination, and at reverse bias, an anodic current (photocurrent) appears. Moreover, it can be seen that the onset potential of the anodic photocurrent (E_{on}) at the polished n-Si electrode is 65 mV more negative than the corresponding one at the SiNW array photoelectrode. In the case of the SiNW array photoelectrode, the photocurrent increases steeply to a plateau region [where the photocurrent is limited by hole production in the semiconductor space-charge region (i.e., by light intensity)], whereas the case of the polished n-Si electrode exhibited an inflection point in the j - E behavior (see Fig. 4). In fact, the j - E curves under illumination of polished n-Si and SiNW electrodes exhibited a sigmoidal and squarelike line shapes, respectively. Moreover, the photocurrent density of the SiNW array photoelectrode is greater than the value for the polished n-Si one at potentials well positive than -0.070 V vs SCE. This suggests that SiNW arrays can harvest light more effectively than polished n-Si photoanodes. Representative PEC output data (i.e., open-circuit potential, V_{oc} ; short-circuit photocurrent density, J_{sc} ; fill factor and conversion

Table I. Averaged PEC J - E data for clean polished n-Si and n-SiNW array electrodes in 0.1/0.1 M $[\text{Fe}(\text{CN})_6]^{4-/3-}$ redox electrolyte under white illumination, 40 mW/cm².

Electrode	V_{oc} (mV)	J_{sc} (mA/cm ²)	Fill factor	Efficiency (%)
Clean polished n-Si	390 ± 10	0.75 ± 0.05	0.21 ± 0.06	0.15 ± 0.06
n-SiNW	323 ± 10	0.89 ± 0.05	0.41 ± 0.06	0.30 ± 0.06

efficiency) from these curves are given in Table I. Uncertainties related to V_{oc} and J_{sc} values include instrumental errors and statistic over 10 measurements. Meanwhile, the uncertainties of fill factor and conversion efficiency were estimated from the corresponding experimental uncertainties of the involved measurements by mathematical propagation.

It can be appreciated that the SiNW array photoelectrodes exhibited a V_{oc} value lower than that of the polished n-Si ones. The last is in agreement of previously reported PEC studies in which nanorod $[\text{Cd}(\text{Se},\text{Te})]^{11}$ and nanowire (Si)¹⁷ array electrodes yielded smaller V_{oc} values than the respective planar ones. Studies on silicon nanorods¹⁶ and silicon nanowires¹⁸ based PEC cells give V_{oc} values greater than the corresponding planar electrode. The low value in V_{oc} for the SiNWs can be related to two factors:¹¹ (i) one inherent to the nanowire array geometry and (ii) one that can, in principle, be manipulated with optimized materials processing and junction formation. The inherent effect takes into account that the SiNW array electrode distributes the photogenerated minority carrier flux over a larger junction collection area than is present for a planar electrode geometry. Therefore, if the charge is collected over the entire SiNW surface and if the rate of production of photogenerated charge-carriers is the same for both SiNW and polished n-Si electrodes, then the minority carrier flux across the junction interface will be less for each nanowire in the SiNW array electrode than is present across the same projected area for the planar polished n-Si junction interface.¹¹ The open-circuit potential is related to the photocurrent density across the junction area by^{11,27,28}

$$V_{\text{oc}} = \left(\frac{kT}{q} \right) \ln \left(\frac{J_{\text{sc}}}{\gamma J_0} \right) \quad [1]$$

where k is Boltzmann's constant, T is the temperature, q is the elementary charge, J_0 is the reverse saturation current density over the actual junction area, J_{sc} is the short-circuit current density per unit of projected device area, and γ is the ratio of the junction area for a nanowire electrode to a planar electrode, which is given by

$$\gamma = \frac{A_{\text{NW}}}{A_{\text{P}}} = \frac{2\pi r h \rho_{\text{NW}} A_{\text{P}}}{A_{\text{P}}} = 2\pi r h \rho_{\text{NW}} \quad [2]$$

where A_{NW} is the junction area of the nanowire array electrode, A_{P} is the area of the planar electrode junction, r is the radius of a single nanowire, h is the height of the nanowires, and ρ_{NW} is the density of nanowires. (Note that this definition of γ only considers the area of the sidewalls of the NWs and neglects the area of the top of the NWs and of the base between NWs). Hence, from Eq. 1, the open-circuit potential of a NW array electrode is related to the open-circuit potential of a planar electrode by the following relationship

$$V_{\text{oc}}^{\text{NW}} = V_{\text{oc}}^{\text{P}} - \left(\frac{KT}{q} \right) \ln \gamma \quad [3]$$

where $V_{\text{oc}}^{\text{NW}}$ and V_{oc}^{P} are the open-circuit potential for a NW array electrode and a planar one, respectively. Therefore, the open-circuit potential will be decreased in NW electrode arrays having $\gamma \gg 1$ relative to the value of the open-circuit potential produced by an analogous absorber and junction in a planar electrode system. For the SiNW arrays used herein, $r \approx 50$ to 80 nm, $h \approx 16$ μm , and $\rho_{\text{NW}} \approx 10^9$ nanowires cm^{-2} ; thus, $\gamma \approx 50$ to 80. Therefore, this γ value will produce a decrease in V_{oc} of ca. 110 mV for the SiNW array electrode relative to the planar electrode, if all other param-

eters are equivalent. In the present case, a decrease in V_{oc} of only ca. 70 mV has been observed, lower than that predicted above, which can be due to the better performance of J_{sc} of the SiNW electrodes relative to the planar ones (see below) and according to Eq. 1. The second factor mentioned above, as a responsibility of the low open-circuit potential exhibited by the SiNW array electrodes, can be assigned to surface or junction recombination, which is more important in systems having a higher junction area per unit of projected area than a planar system. However, this last factor can, in principle, be solved and obtain an increase of the V_{oc} for such systems by increasing the doping of the nanowires, or lowering the J_0 of the solid-liquid contact.¹⁷ The SiNW array electrodes exhibited, however, higher overall short-circuit current densities (J_{sc}) than the polished planar n-Si electrodes (see Table I). The last is in line with previously published works.^{16,18} This J_{sc} value obtained herein for the SiNW array photoelectrodes is 250% greater than the better J_{sc} value reported in the literature for similar SiNW array photoelectrodes normalized at a light intensity of 100 mW/cm².¹⁸ J_{sc} provides information on the net quantum yield for charge separation and also serves as a measure of the yield of minority carriers that survive the cross of the solid-liquid interface.²⁹ This enhancement in the photocurrent of the SiNW photoelectrodes compared to the planar polished n-Si ones can be due to the excellent antireflective ability of the SiNW arrays and to a better collection of minority carriers. Moreover, the SiNW arrays exhibited better fill factors than the planar n-Si samples investigated in the present study (see Table I). This fact can, in principle, be attributable to an improved ratio of charge-transfer relative to surface recombination, as a result of increasing the internal junction area.¹¹ The optimization of PEC efficiency required not only high J_{sc} values but also high values of the fill factor.²⁹ Furthermore, the overall efficiency of the SiNW array photoelectrodes is approximately twice those of planar n-Si junction devices (see Table I). The uncertainties on the fill factor and efficiency values were estimated, as it was said above, by mathematical propagation from the corresponding experimental uncertainties of the involved measurements. Moreover, the tabulated uncertainties are absolute values being the corresponding relative values the following: ca. 30% for fill factor, ca. 40% for conversion efficiency in the case of the clean polished Si electrodes; while ca. 15% for fill factor and ca. 20% for the efficiency in the case of the n-SiNW ones. Furthermore, these relative error values are in agreement with those reported in the literature for similar PEC procedure and measurements, for instance, Spurgeon et al.¹¹ reported relative errors of 14% on fill factor and a mean value of 30% for the relative error on the conversion efficiency.

As the kinetic traces of the photocurrent generated on intermittent illumination can give some approaching into the electronic properties of the semiconducting photoelectrodes,³⁰ the PEC properties of the n-Si and SiNW electrodes were studied in more detail by time-resolved photocurrent measurements. Depending on the photoelectrode potential, the photocurrent transient response of the electrode varies significantly. Typical examples measured at $E = 0.0$ V vs SCE for n-Si and SiNW array photoelectrodes are given in Fig. 5. In the case of the n-Si electrodes, after the beginning of the illumination, a large anodic photocurrent peak attributed to bulk separation of photogenerated electrons and holes pairs appears. Immediately, a photocurrent decay due to electrons and holes surface recombination or band-bending decrease is observed until a station-

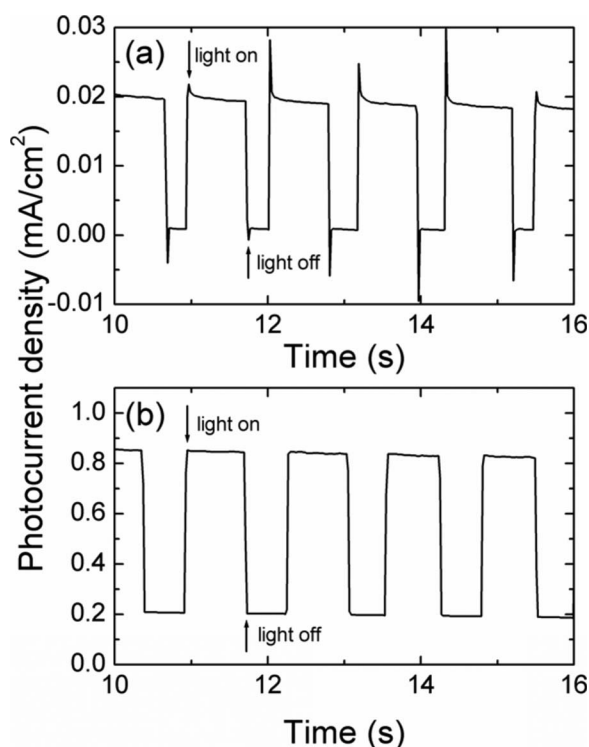


Figure 5. Photocurrent transients of (a) n-Si and (b) n-Si nanowire array photoelectrodes under polarization at $E = 0.0$ V vs SCE, in 0.5 M KNO_3 + 0.1 M $\text{K}_3\text{Fe}(\text{CN})_6$ + 0.1 M $\text{K}_4\text{Fe}(\text{CN})_6$ solution, under white illumination (40 mW/cm²).

ary photocurrent is attained (see Fig. 5a). Moreover, the overshoots of the photocurrents and their subsequent decay toward a steady-state value indicate a significant accumulation of holes at the electrode surface under illumination. When light is switched off, cathodic currents were observed before the dark value was reached again, which can be attributed to the recombination of these surface-trapped holes with electrons from the conduction band of Si. In the case of the SiNW photoelectrodes, and at the same polarization potential, a “square” photoresponse was observed (see Fig. 5b) (the anodic photocurrent transient disappears), the last indicating a different band bending and a better separation way of the photogenerated electrons and holes pairs.

Conclusions

Vertically aligned arrays of high aspect single-crystalline n-SiNWs have been synthesized by electroless metal deposition on a silicon wafer chip in an ionic silver HF solution through selective etching under standard pressure. The SiNW samples are dark black in appearance. The absolute reflectance of the SiNW is $<1\%$ for almost all treated samples. Their PEC properties were measured and compared to those of its untreated bare polished Si sample counterpart. The open-circuit photovoltage, V_{OC} , short-circuit current density, J_{SC} , fill factor, and overall energy conversion efficiency for

both types of electrodes was measured under 40 mW cm⁻² white illumination conditions. V_{OC} was lower, on average, for SiNWs array photoelectrodes, while J_{SC} , fill factor and overall efficiencies of the SiNWs array photoelectrodes were generally superior to those of the bare polished Si junction devices.

Acknowledgments

The authors are grateful to Universidad de Málaga, Málaga, Spain, for the financial support received. E.A.D. and R.E.M. also acknowledge the financial support of PEDECIBA-Física, and especially to C.S.I.C., Universidad de la República, Montevideo, Uruguay. The authors also thank A. Martínez Orellana and Gregorio Martín (Málaga, Spain) for SEM and TEM measurements.

Universidad de la República and Universidad de Málaga assisted in meeting the publication costs of this article.

References

1. L. J. Chen, *J. Mater. Chem.*, **17**, 4639 (2007).
2. B. K. Teo and X. H. Sun, *Chem. Rev. (Washington, D.C.)*, **107**, 1454 (2007).
3. J.-J. Wu, G.-R. Chen, H.-H. Yang, C.-H. Ku, and J.-Y. Lai, *Appl. Phys. Lett.*, **90**, 213109-1 (2007).
4. J. Tornow and K. Schwarzburg, *J. Phys. Chem. C*, **111**, 8692 (2007).
5. E.-C. Cho, S. Park, X. Hao, D. Song, G. Conibeer, S.-C. Park, and M. A. Green, *Nanotechnology*, **19**, 245201 (2008).
6. K. Peng, Z. Huang, and J. Zhu, *Adv. Mater. (Weinheim, Ger.)*, **16**, 73 (2004).
7. L. Tsakalakos, J. Balch, J. Fronheiser, B. A. Korevaar, O. Sulima, and J. Rand, *Appl. Phys. Lett.*, **91**, 233117 (2007).
8. B. Tian, X. Zheng, T. J. Kempa, Y. Fang, N. Yu, G. Yu, J. Huang, and C. M. Lieber, *Nature (London)*, **449**, 885 (2007).
9. R. Tena-Zaera, M. A. Ryan, A. Katty, G. Hodes, S. Bastide, and C. Lévy-Clément, *C. R. Chim.*, **9**, 717 (2006).
10. J. B. Baxter and E. S. Aydil, *Appl. Phys. Lett.*, **86**, 053114 (2005).
11. J. M. Spurgeon, H. A. Atwater, and N. S. Lewis, *J. Phys. Chem. C*, **112**, 6186 (2008).
12. B. M. Kayes, H. A. Atwater, and N. S. Lewis, *J. Appl. Phys.*, **97**, 114302 (2005).
13. B. M. Kayes, C. E. Richardson, N. L. Lewis, and H. A. Atwater, in *Conference Record of the Thirty-first IEEE Photovoltaic Specialists Conference*, p. 55 (2005).
14. S. U. M. Khan and T. Sultana, *Sol. Energy Mater. Sol. Cells*, **76**, 211 (2003).
15. Th. Stelzner, M. Pietsch, G. André, F. Falk, E. Ose, and S. Christiansen, *Nanotechnology*, **19**, 295203 (2008).
16. J. R. Maiolo, B. M. Kayes, M. A. Filler, M. C. Putnam, M. D. Kelzenberg, H. A. Atwater, and N. S. Lewis, *J. Am. Chem. Soc.*, **129**, 12346 (2007).
17. A. P. Goodey, S. M. Eichfeld, K.-K. Lew, J. M. Redwing, and T. E. Mallouk, *J. Am. Chem. Soc.*, **129**, 12344 (2007).
18. K. Peng, X. Wang, and S.-T. Lee, *Appl. Phys. Lett.*, **92**, 163103 (2008).
19. K.-Q. Peng, Y.-J. Yan, S.-P. Gao, and J. Zhu, *Adv. Mater. (Weinheim, Ger.)*, **14**, 1164 (2002).
20. E. A. Dalchiele, F. Martín, D. Leinen, R. E. Marotti, and J. R. Ramos-Barrado, *Thin Solid Films*, Submitted.
21. A. I. Hochbaum, R. Chen, R. D. Delgado, W. Liang, E. C. Garnett, M. Najarian, A. Majumdar, and P. Yang, *Nature (London)*, **451**, 163 (2008).
22. G.-H. Ding, C. T. Chan, Z. Q. Zhang, and P. Sheng, *Phys. Rev. B*, **71**, 205302 (2005).
23. L. Hu and C. Cheng, *Nano Lett.*, **7**, 3250 (2007).
24. Y. W. Chen, D. Cahen, R. Noufi, and J. A. Turner, *Sol. Cells*, **14**, 109 (1985).
25. M. S. Wrighton, A. B. Bocarsly, J. M. Bolts, A. B. Ellis, and K. D. Legg, in *Semiconductor Liquid-Junction Solar Cells*, A. Heller and M. Hill, Editors, PV 77-3, pp. 138-156, The Electrochemical Society Proceedings Series, Pennington, NJ (1977).
26. M. J. Madou, B. H. Loo, K. W. Frese, and S. R. Morrison, *Surf. Sci.*, **108**, 135 (1981).
27. K. Rajeshwar, in *Encyclopedia of Electrochemistry*, A. J. Bard, M. Stratmann, and S. Licht, Editors, Vol. 6, Wiley-VCH, Weinheim (2002).
28. S. M. Sze, *Physics of Semiconductor Devices*, John Wiley & Sons, Inc., New York (1969).
29. N. S. Lewis, *Acc. Chem. Res.*, **23**, 176 (1990).
30. J. J. Ramsdell and R. Tóth-Boconádi, *J. Chem. Soc., Faraday Trans.*, **86**, 1527 (1990).